ISSN 1062-8738, Bulletin of the Russian Academy of Sciences. Physics, 2014, Vol. 78, No. 10, pp. 1030–1034. © Allerton Press, Inc., 2014.
Original Russian Text © M.S. Blanter, V.V. Dmitriev, A.V. Ruban, 2014, published in Izvestiya Rossiiskoi Akademii Nauk. Seriya Fizicheskaya, 2014, Vol. 78, No. 10, pp. 1282–1286.

Ordering in V–O and V–N Solid Solutions: Computer Simulation

M. S. Blanter[a], **V. V. Dmitriev**[a], **and A. V. Ruban**[b]

[a] *Moscow State University of Instrumental Engineering and Informatics, Moscow, 107996 Russia*
[b] *Department of Material Science and Engineering, Royal Institute of Technology, SE-10044 Stockholm, Sweden*
e-mail: mike.blanter@gmail.com

Abstract—The atomic structures of interstitial solid solutions O and N in V at relatively low concentrations O(N)/V = 1/16 or 1/8 are calculated using the Monte Carlo method. A combined model of long-range interaction between interstitial atoms is employed. The first 12 shells contain ab initio energies and the energies in shells 13–18 are calculated on the basis of a phenomenological model of deformation interaction. The ordered solid solutions are long-period structures with body-centered tetragonal crystal lattices and tetragonality $c/a < 1$.

DOI: 10.3103/S1062873814100050

INTRODUCTION

Interactions between dissolved atoms determine the short- and long-range orders in interstitial solid solutions. For solutions with relatively weak interactions between interstitial atoms (e.g., O in HCP metals (α-Ti,Zr,Hf)), the experimental data on superstructures are consistent [1, 2] and coincide with calculations [3]. For solid solutions with strong interaction between interstitial atoms (O and N in BCC metals of V, Nb, and Ta), the experimental data are contradictory [4–7]. For V–O and V–N alloys with relatively low concentrations O(N)/V = 1/16–1/8 in particular, several phases released from the solid solution as a result of different thermal treatments were reported in [6–14]. According to the authors, most of these phases are metastable and can be ordered solid solutions with both BCC or BCT structures or other (e.g., FCC or hexagonal) lattices. The last structures can also be formed by ordering the interstitial solid solution. However, when there are strong displacements of metal atoms around interstitial atoms (particularly the atoms of O and N in V considered in this work) deformation transitions to BCT, FCC, hexagonal, orthorhombic, and other structures occurs during ordering in the initial crystal lattice of the solvent metal [15]. This leads to the formation of other phases that differ from simply ordered BCC or BCT solid solutions at relatively high concentrations of the solid solution (O(N)/V = 1/4–1) in these alloys [6, 7, 15].

The content of ordered structures is usually determined by the average concentration of interstitial atoms in an alloy, but only when all of the solid solution is converted to the ordered phase. However, another situation is observed due to the low solubility of oxygen and nitrogen in vanadium [6, 7], particularly at room temperature: particles of the ordered phase are liberated from a solid solution when its content can differ from that of the initial solution. An alternative to this is determining the content from the structure of ordered phase using experimental diffraction data. However, this method can lead to confusion, since modeling atomic structures solely on the basis of diffraction data does not always yield clear results.

Another technique for studying the atomic structure of ordered solid solutions is to perform calculations using different theories of interaction between interstitial atoms [16]. In such calculations, it is assumed that the superstructure is formed by the redistribution of interstitial atoms over the octahedral or tetrahedral interstices of a metal-dissolvent initial lattice until the minimum of the internal configuration or free energy is attained. For solid solutions with relatively weak interaction between interstitial atoms—H in V, Nb, Ta [17] or O in α-Ti, Zr, Hf [3]—such calculations agree well with the experimental data. In the former case, the energies of interstitial atom interactions can be calculated using the phenomenological theory of deformation (elastic) interaction [16]; in the latter, we can apply ab initio principles in the context of density functional theory.

The energies of interaction between interstitial atoms, as determined by ab initio calculations in 12 coordination spheres in the context of density functional theory, were given in [18] for solid solutions of O and N in V, Nb and Ta. It was also shown that an adequate description of the behavior of interstitial atoms can be obtained using a combined model in which these ab initio energies of interaction in the first 12 coordination shells are added to those in shells 13–18 through deformation interaction, calculated on the basis of the phenomenological model [19]. Such an approach allows us to consider the long-range character of interaction, which is almost impossible to do in ab initio calculations because of the excessive time required for calculations.

It is of interest to study the structure of ordered solid solutions in the context of the model of long-range interaction between interstitial atoms. In this work, such calculations are performed for interstitial solid solutions of O and N in V with relatively low concentrations: O(N)/V = 1/16 or 1/8.

CALCULATION PROCEDURE

The energies of O–O and N–N interatomic pair interaction in the first 12 coordination shells were taken from [18] (the distance between interstitial atoms was from 0.5 to 1.803 *a*, where *a* is the period of BCC crystal lattice of vanadium). They were calculated on the basis of the density functional theory using the VASP software and included both chemical and deformation (elastic) contributions. In spheres 13–18 (1.870–2.236 *a*), we used energies of deformation interaction calculated in the context of the phenomenological Krivoglaz–Kanzaki–Khachaturyan model [16] presented in [19]. The energies in the 18 coordination shells are shown in Table 1.

The crystal structure was calculated using the Monte Carlo method in a $12 \times 12 \times 12\ a^3$ BCC model cell with periodic boundary conditions. One aspect of our calculations was that the transitions of interstitial atoms were considered not only in the nearest octahedral interstices but in any that were free. The configuration's contribution to heat capacity *C* was calculated from the temperature dependence of the internal configuration energy.

In an BCC crystal lattice, the octahedral interstices form three sublattices, *x*, *y*, and *z*, in which the two atoms closest to the interstice are located along axis *x*, *y*, and *z*, respectively. When one of the sublattices is filled in, the lattice parameter increases along the corresponding direction *x*, *y*, or *z* and decreases along the two others. If the three sublattices of an octahedral interstice are not equally filled with interstitial atoms, we see tetragonality, and the sublattice becomes a body-centered tetragonal. When the concentration in one sublattice exceeds that in the other two, the tetragonality is $c/a > 1$; otherwise, it is $c/a < 1$. This parameter is determined in most experimental papers and can be used to compare calculations with experimental data.

Long-range order parameters α were determined from sublattice filling with the maximum concentration of interstitial atoms:

$$a = (p - p_{\mathrm{av}})/(p_{\max} - p_{\mathrm{av}}), \qquad (1)$$

where *p* is the probability of interstice filling for given sublattice, $p_{\max}$ is the maximum probability, and p_{av} is the average probability at a given concentration.

RESULTS AND DISCUSSION

The temperature dependence of the heat capacity (Fig. 1) and long-order parameters (Fig. 2) indicate ordering occurred in the investigated alloys. The temperature of the heat capacity's maximum and the temperature below which the long-order parameters began to increase were both taken as the ordering temperature (Kurnakov temperature T_C). Temperatures T_C determined from the two characteristics (Table 2) were in very good agreement, especcially when we consider that the calculations were performed with steps of 20°.

Table 1. Energies of pair interaction between interstitial atoms [18,19] (positive energies correspond to repulsion)

Shell number	$2r/a$	$\lvert r\rvert/a$	V–O	V–N
1	010	0.5	+1.53	–0.02
2	011	0.707	+0.85	+0.84
3	111	0.866	+0.27	+0.15
4a	020	1.0	+0.05	–0.02
4b	002	1.0	+1.59	+1.50
5	210	1.118	+0.06	–0.05
6	121	1.225	+0.09	0.00
7a	220	1.414	+0.10	+0.04
7b	202	1.414	+0.11	+0.10
8a	212	1.5	+0.12	+0.11
8b	030	1.5	–0.03	–0.04
9	103	1.581	+0.11	+0.06
10a	311	1.658	0.00	0.00
10b	113	1.658	+0.16	+0.15
11	222	1.732	0.00	–0.01
12	230	1.803	0.00	–0.03
13	321	1.871	+0.01	0.00
14a	400	2.000	–0.03	–0.02
14b	004	2.000	+0.16	+0.18
15a	410	2.062	–0.04	–0.05
15b	232	2.062	–0.03	–0.02
16a	141	2.121	0.00	0.00
16b	303	2.121	0.00	+0.02
17a	331	2.179	+0.02	+0.01
17b	313	2.179	–0.02	–0.03
18a	420	2.236	–0.01	–0.01
18b	024	2.236	+0.01	+0.01
18c	402	2.236	0.00	0.00

The ordering temperatures for all four alloys were above room temperature; i.e., ordered structures formed upon the rather slow cooling to room temperature at which the experimental data were obtained.

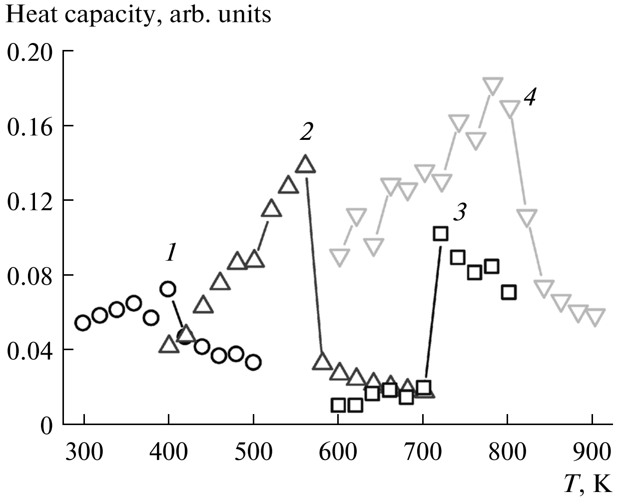

Fig. 1. Changes in the configuration part of heat capacity upon the cooling of alloys: (*1*, *3*) V–O; (*2*, *4*) V–N. Concentrations: (*1*, *2*) O(N)/V = 1/16; (*3*, *4*) 1/8.

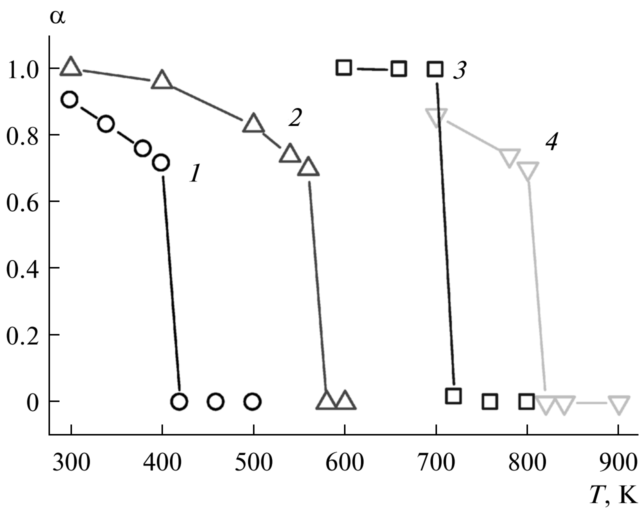

Fig. 2. Changes in long-order parameters upon the cooling of alloys: (*1*, *3*) V–O; (*2*, *4*) V–N. Concentrations: (*1*, *2*) O(N)/V = 1/16; (*3*, *4*) 1/8.

At the same time, the degree of order was high: the long-order parameter was $\alpha = 0.9$ at 300 K in $V_{16}O$ alloy and $\alpha = 1$ for other alloys. T_C rose with growing concentration and was higher in nitrogen-containing alloys, due possibly to the interaction in the first coordinate shells differing substantially (Table 1): it was strongly repulsive in V–O but weakly attractive in V–N.

Modeling showed that small isolated clusters of interstitial atoms do not form, as is usually assumed when describing solutions with such relatively low concentrations; rather, there were solid areas of ordered solid solution. Our model superstructures are depicted in Figs. 3–5. They are all long-periodic in two directions with periods of $4a$ or $3a$, while the third period is $1a$, where a is the period of the BCC lattice of vanadium (Table 2). The concentrations of superstructures in alloys where O(N)/V = 1/16 was higher than the average alloy concentrations: 1/8 for V–O and 1/6 for V–N, respectively. An ordered solid solution with a higher concentration of interstitial atoms occupied part of our model crystal, forming flat clusters whose sizes matched those of a model crystal in two dimensions and were half the size in the third. Our initial solid solution thus separated into a pure metal and an ordered solid solution. Ordered V_6O and V_8N phases were formed in alloys where O(N)/V = 1/8. In these cases, virtually all of the solid solution became ordered and occupied all or almost all of a model crystal.

In all four alloys, two sublattices of octahedral interstices were occupied in the ordered BCC solid solution, while the third was completely free. Since the crystal lattice is stretched biaxially and compressed along the third axis when two sublattices are filled with interstitial atoms, tetragonality results with $c/a < 1$.

Shortening the range of interaction between interstitial atoms from 18 to 12 coordinate shells (from 2.236 to 1.803 a), i.e., performing calculations with only the ab initio energies of interactions, produces

Table 2. Characteristics of interstitial ordered solid solutions of V–O and V–N

Alloy	V–O		V–N	
Concentration O(N)/V	1/16	1/8	1/16	1/8
Ordering temperature, K (heat capacity)	400	720	560	780
Ordering temperature, K (long-order parameter)	400	700	560	800
Periods of superstructure	4 × 4 × 1	4 × 4 × 1	4 × 3 × 1	4 × 3 × 1
Content of ordered phase	V_8O	V_8O	V_6N	V_8N
Tetragonality c/a	<1	<1	<1	<1

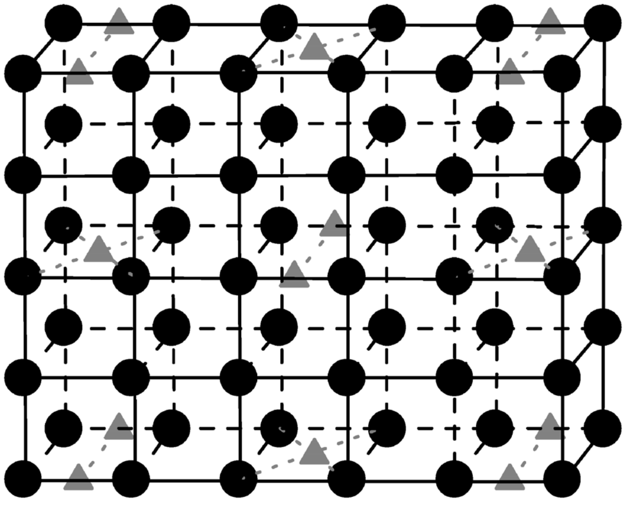

Fig. 3. Atomic structure of ordered solid solution in V–O alloys with O/V contents of 1/16 and 1/8. Circles are vanadium atoms; triangles are oxygen atoms. For clarity, vanadium atoms in the centers of BCC cells are not shown.

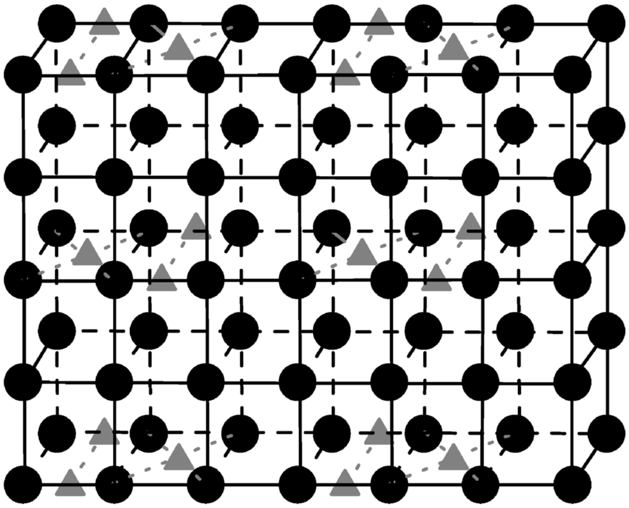

Fig. 4. Atomic structure of an ordered solid solution in V–N alloy with an N/V content of 1/16. Circles are vanadium atoms; triangles are nitrogen atoms. For clarity, vanadium atoms in the centers of BCC cells are not shown.

fuzzy ordered structures with almost the same degree of filling for all three sublattices of the octahedral interstices. No tetragonality is observed, but there is a maximum of heat capacity that indicates ordering; however, temperatures T_C are much lower than for 18 spheres. This can be explained by the mutual attraction between interstitial atoms in shells 13–18.

It is difficult to compare the results obtained in this work with results from experiments, since most experimental phases are nonequilibrium and only a few structures were presented in [8–14]. Even though none of our calculated structures coincide with ones proposed on the basis of experimental diffraction data, several general features of our structures are in good agreement with those of experimental results:

(i) Some experimentally investigated vanadium-based oxides and nitrides were ordered solid solutions, as was demonstrated by the presence of superstructure reflections, and these solutions had body-centered tetragonal lattices. Using our model of interaction between interstitial atoms, calculations also reveal ordering even at relatively low concentrations of a solid solution.

(ii) Most of the studied solid solutions, whether they were equilibrium or not, had BCT structures with tetragonality $c/a < 1$, as was found in our calculations.

(iii) In some reference works [10, 11], experimental data suggest the existence of long-periodic structures with $4 \times 4 \times 1a^3$ cells, as do our results.

The discrepancy between our simulated structures and those reconstructed on the basis of experimental data is apparently due to the calculated structures are equilibrium, while experimental ones seem to be metastable. To some extent, our calculation results prove the suggestion of many authors that V–O and V–N phases investigated in dilute alloys are metastable.

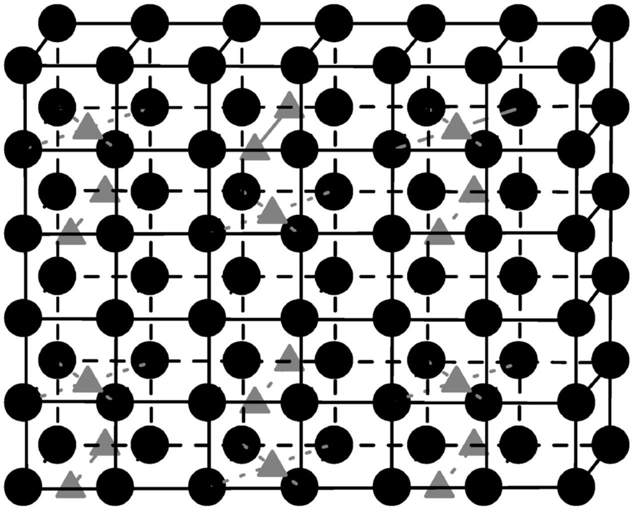

Fig. 5. Atomic structure of an ordered solid solution in V–N alloy with an N/V content of 1/8. Circles are vanadium atoms; triangles are nitrogen atoms. For clarity, vanadium atoms in the centers of BCC cells are not shown.

CONCLUSIONS

Modeling interstitial superstructures in dilute V–O and V–N alloys using the model of long-range interaction between interstitial atoms reveals the formation of continuous areas of ordered solutions with concentrations higher than or equal to those of the initial disordered solutions. Ordered solid solutions are long-periodic structures with face-centered tetragonal crystal lattices and tetragonality $c/a < 1$.

REFERENCES

1. Tsuji, T., *J. Nucl. Mat.*, 1997, vol. 247, pp. 63–71.
2. Yamaguchi, S., Hiraga, K., and Hirabayashi, M., *J. Phys. Soc. Jpn.,* 1970, vol. 28, pp. 1014–1023.
3. Ruban, A.V., Baykov, V.I., Johansson, B., et al., *Phys. Rev. B*, 2010, vol. 82, p. 134110/1-10.
4. Hong, H.S. and Lee, K.S., *J. Alloys Compounds*, 2003, vol. 360, pp. 198–204.
5. Garg, S.P., Krishnamurthy, N., Awasthi, A., and Venkatraman, M., *Phase Diagram Evaluations: Sect. II*, 1996, vol. 17, pp. 63–77.
6. Alcock, C.B. and Ji, C., *High Temp., High Pressure*, 1990, vol. 22, pp. 139–147.
7. Carlson, O.N., Smith, J.E., and Hafziger, R.H., *Metall. Trans. A*, 1986, vol. 17, pp. 1647–1656.
8. Potter, D.I., Epstein, H.D., and Goldstein, B.M., *Met. Trans.*, 1974, vol. 5, pp. 2075–2085.
9. Potter, D.I. and Altstetter, C., *Acta Metall.*, 1972, vol. 20, pp. 313–318.
10. Potter, D.I. and Altstetter, C., *Scripta Met.*, 1970, vol. 4, pp. 849–852.
11. Potter, D.I. and Altstetter, C., *Acta Metall.*, 1971, vol. 19, pp. 881–886.
12. Henry, J.L., O'Hare, S.A., McCune, R.A., and Krug, M.P., *J. Less-Common Met.,* 1970, vol. 21, pp. 115–135.
13. Gunwalden, D. and Potter, D., *J. Less-Common Met.,* 1974, vol. 34, pp. 97–106.
14. Nouet, G., Vicens, J., and Delavignette, P., *Phys. Status Solidi A*, 1980, vol. 62, pp. 449–457.
15. Somenkov, V.A., Irodova, A.V., and Shilshtein, S.Sh., *Solid State Phys.,* 1978, vol. 20, pp. 3076–3083.
16. Khachaturyan, A.G., *Theory of Structural Transformations in Solids,* New York: Wiley, 1983.
17. Khachaturyan, A.G. and Shatalov, G.A., *Acta Metall.,* 1975, vol. 23, pp. 1089–1102.
18. Blanter, M.S., Dmitriev, V.V., and Ruban, A.V., *J. Phys. Chem. Solids*, 2013, vol. 74, pp. 716–722.
19. Blanter, M.S. and Khachaturyan, A.G., *Metall. Trans. A*, 1978, vol. 9, pp. 753–762.

Translated by O. Maslova